Journal of Reproduction and Development, Vol. 66, No 4, 2020

—Original Article—

Ruthenium red improves blastocyst developmental competence by regulating mitochondrial Ca^{2+} and mitochondrial functions in fertilized porcine oocytes *in vitro*

Ho-Geun JEGAL[1, 2)*], Hyo-Jin PARK[1, 2)*], Jin-Woo KIM[1, 2)], Seul-Gi YANG[1, 2)], Min-Ji KIM[1, 2)] and Deog-Bon KOO[1, 2)]

[1)]*Department of Biotechnology, College of Engineering, Daegu University, Gyeongbuk 38453, Republic of Korea*
[2)]*Institute of Infertility, Daegu University, Gyeongbuk 38453, Republic of Korea*

Abstract. Ruthenium red (RR) inhibits calcium (Ca^{2+}) entry from the cytoplasm to the mitochondria, and is involved in maintenance of Ca^{2+} homeostasis in mammalian cells. Ca^{2+} homeostasis is very important for further embryonic development of fertilized oocytes. However, the effect of RR on mitochondria-Ca^{2+} (mito-Ca^{2+}) levels during *in vitro* fertilization (IVF) on subsequent blastocyst developmental capacity in porcine is unclear. The present study explored the regulation of mito-Ca^{2+} levels using RR and/or histamine in fertilized oocytes and their influence on blastocyst developmental capacity in pigs. Red fluorescence intensity by the mito-Ca^{2+} detection dye Rhod-2 was significantly increased ($P < 0.05$) in zygotes 6 h after IVF compared to mature oocytes. Based on these results, we investigated the changes in mito-Ca^{2+} by RR (10 and 20 μM) in presumptive zygotes using Rhod-2 staining and mito-Ca^{2+} uptake 1 (MICU1) protein levels as an indicator of mito-Ca^{2+} uptake using western blot analysis. As expected, RR-treated zygotes displayed decreased protein levels of MICU1 and Rhod-2 red fluorescence intensity compared to non-treated zygotes 6 h after IVF. Blastocyst development rate of 20 μM RR-treated zygotes was significantly increased 6 h after IVF ($P < 0.05$) due to improved mitochondrial functions. Conversely, the blastocyst development rate was significantly decreased in histamine (mito-Ca^{2+} inhibitor, 100 nM) treated zygotes ($P < 0.05$). The collective results demonstrate that RR improves blastocyst development in porcine embryos by regulating mito-Ca^{2+} and MICU1 expression following IVF.

Key words: *In vitro* fertilization, Mito-Ca^{2+} uptake 1 (MICU1), Mitochondria-Ca^{2+}, Porcine embryos, Ruthenium red

(**J. Reprod. Dev. 66:** 377–386, 2020)

During early embryonic development, mito-Ca^{2+} uptake is closely associated with mitochondrial functions in mice [1]. The accumulation of mito-Ca^{2+} caused mitochondrial depolarization through changes in mitochondrial membrane potential (MMP), leading to mitochondrial dysfunction [2]. Excessive mito-Ca^{2+} also causes DNA fragmentation by releasing mitochondrial apoptotic factors during *in vitro* maturation (IVM) [3]. Induction of mitochondrial dysfunctions by accumulating mito-Ca^{2+} in preimplantation embryos contributes to the activation of mitochondria-mediated apoptosis pathways [4]. However, it is not clear whether mito-Ca^{2+} related mechanisms affect early embryonic development in pigs.

The increasing cytoplasm Ca^{2+} level between adjoining domains of the endoplasmic reticulum (ER) and mitochondria allows mito-Ca^{2+} uptake. These responses increase mito-Ca^{2+} through the transfer of Ca^{2+} from the ER to the cytoplasm [5]. The mito-Ca^{2+} uniporter (MCU) is a Ca^{2+}-selective channel located in the mitochondrial inner membrane in HeLa cells [6]. The discovery of the MCU complex, which is a calcium-selective channel in mitochondria inner membrane, revealed that mitochondria absorb cytoplasmic Ca^{2+} [7]. However, it is not clear whether the presence of functions of the MCU complex via mito-Ca^{2+} related mechanisms affect the fertilization and early embryonic development in pigs. Mitochondria of mouse oocytes regulate the release of Ca^{2+} from the ER to the cytoplasm during IVF [8]. A recent study demonstrated that the modulation of mito-Ca^{2+} homeostasis in mature oocytes plays a fundamental role in cytoplasmic maturation during IVM [9]. In addition, the mito-Ca^{2+} level regulates mitochondrial functions, mitochondria dynamics, and mitochondria-mediated apoptosis in mammals [10]. Therefore, regulation of mito-Ca^{2+} production plays an important role in fertilization and maintenance of mitochondrial functions in blastocyst formation during early embryonic development. Therefore, it seems that the regulation of mito-Ca^{2+} or Ca^{2+} homeostasis in mitochondria has a well-designed mechanism during IVF, which might effectively control the fertilization rate and further capability of embryo development.

Rhod-2 is a mito-Ca^{2+}-specific detection dye with a positive charge. The dye can enter mitochondria. Rhod-2 is also a staining reagent that detects Ca^{2+} in mitochondria via MMP [11]. Changes in mito-Ca^{2+} by Rhod-2 staining are involved in cellular apoptosis and cytoplasm maturation of oocytes in obese mice [12]. In addition, we previously described the relationship between morphological quality

Received: January 29, 2020
Accepted: April 12, 2020
Advanced Epub: April 22, 2020

Correspondence: D-B Koo (e-mail address: dbkoo@daegu.ac.kr)
* H-G Jegal and H-J Park contributed equally to this work.

and red fluorescence expression levels of Rhod-2 in the detection of mito-Ca^{2+} in mature oocytes and presumptive zygotes [13]. Our data suggested that the changes in Rhod-2 expression pattern could be used as a quality criterion in mature porcine oocytes and zygotes.

RR blocks Ca^{2+} in the cytoplasm from entering mitochondria via MCU in guinea-pig isolated ventricular heart cells [14]. Accordingly, we investigated whether the changes in Rhod2 fluorescence expression by RR for IVF progression have positive effects on further embryonic development in pigs. However, which aspect of RR regulation of mito-Ca^{2+} level during IVF affects porcine embryo development is unknown. Furthermore, the influence of the regulation of mitochondrial functions by the RR-mediated reduction of mito-Ca^{2+} levels during IVF on subsequent developmental competence to the blastocyst stage has not been studied in porcine embryos.

In the present study we investigated the relationship between RR-mediated reduction of mito-Ca^{2+} levels 6 h following IVF and subsequent blastocyst development capacity in pigs (Supplementary Fig. 1: online only). We also confirmed the correlation of mitochondrial functions, such as MMP and ATP, in fertilized oocytes according to different concentrations of RR used in treatment. Finally, we investigated whether the inhibition of mito-Ca^{2+} levels in mitochondria using histamine in porcine fertilized oocytes effectively controlled preimplantation embryo development.

Materials and Methods

Chemicals

Unless otherwise stated, all chemicals and reagents used were purchased from Sigma-Aldrich (St. Louis, MO, USA).

IVM

Porcine ovaries were obtained from 6 months old of female pigs (Yorkshire/Landrace (♀) × Duroc (♂), 100 kg) at the local abattoirs (Gyeongsan and Daegu City, Korea) and transported to the laboratory (Daegu University) in a thermos containing 0.9% saline supplemented with 75 μg/ml potassium penicillin G at approximately 30–35ºC. All procedures in this experiment were approved by the Animal Care and Use Committee of Daegu University and performed in according with animal and ethics. Immature cumulus-oocyte complexes (COCs) were aspirated from follicles (3–6 mm in diameter) using a 10 ml syringe with an 18-gauge needle. The undamaged COCs with a similar cytoplasm quality and surrounding cumulus cells were selected by mouth pipetting and then washed three times in Tyrode's lactate-N-2-hydroxyethylpiperazine-N'2-ethanesulfonic acid (TL-HEPES) medium. Approximately 50 to 60 immature COCs were cultured in 500 μl of IVM medium in a four-well multi-dish at 38.5ºC in 5% CO_2 after three washes in TL-HEPES and IVM medium. Bovine serum albumin (BSA) free North Carolina State University (NCSU)-23 medium supplemented with 10% follicular fluid (v/v), 0.57 mM cysteine, 25 μM β-mercaptoethanol, 10 ng/ml epidermal growth factor (EGF), 10 IU/ml pregnant mare's serum gonadotropin (PMSG) and 10 IU/ml human chorionic gonadotropin (hCG) was used for oocyte maturation [15]. After culturing for 22 h (IVM I), the same media was used for oocyte maturation without PMSG/hCG for 22–44 h (IVM II).

In vitro fertilization (IVF) and culture

IVF of porcine oocytes was performed as described previously [16]. The IVF medium used was modified Tris-buffered medium (mTBM) consisting of 113.1 mM NaCl, 3 mM KCl, 7.5 mM $CaCl_2$, 5 mM sodium pyruvate, 11 mM glucose, 20 mM Tris, 2.5 mM caffeine sodium benzoate, and 1 mg/ml BSA. During the IVF periods (3 or 6 h), RR (5, 10, 20, and 40 μM) and histamine (100 nM) were added to the mTBM to regulate mito-Ca^{2+} levels in porcine oocytes (Supplementary Fig. 2: online only). Fresh semen was kindly supplied by the Darby Porcine AI Center (Anseong, Korea) each week, and stored at 17°C for 2 to 3 days. Semen was washed three times by centrifugation with phosphate buffered saline (PBS) supplemented with 1 mg/ml BSA, 0.37 mg/ml penicillin G, 0.03 mg/ml streptomycin sulfate, and 0.1 mg/ml $CaCl_2$. After the final wash, spermatozoa were re-suspended in mTBM at pH 7.8. Mature oocytes were denuded by gently pipetting in 0.1% hyaluronidase (w/v) and were washed three times in mTBM. Diluted spermatozoa (2 μl) were added to a 48-μl drop of IVF medium containing 20 oocytes to give a final concentration of 1.5×10^5 sperm/ml. Finally, non-treated, RR-treated (5, 10, 20, and 40 μM) or histamine-treated (100 nM) sample was added to the 48 μl drop of IVF medium containing the 20 oocytes and co-incubated with 2 μl of prepared spermatozoa for 6 h at 38.5ºC in an atmosphere of 5% CO_2. In the next experiment, 25 to 30 embryos were cultured in 50 μl drops of IVC medium (PZM-3 containing 3 mg/ml BSA) at 38.5ºC and 5% CO_2. After 48 h of culture, cleaved embryos were further cultured in 50 μl drops of IVC medium at 38.5ºC and 5% CO_2 for 4 days. Blastocyst formation was evaluated after 6 days of culture.

Rhod-2 and Mito-Tracker, Mito-SOX fluorescence staining

To evaluate mito-Ca^{2+} levels in maturated and fertilized oocytes, we performed fluorescence staining using Rhod-2 AM (ab142780; Abcam, Cambridge, MA, USA) as a specific mitochondria calcium detection dye. To identify Rhod-2 fluorescence expression in mature oocytes (44 h after IVM) and fertilized oocytes (3 h or 6 h after IVF), oocytes were washed with 0.1% PBS-polyvinyl alcohol (PVA) and incubated in the dark at 38.5ºC and 5% CO_2 for 15 min in IVF medium supplemented with 100 μM Rhod-2 dye. After Rhod2 treatment, oocytes were washed three times in 0.1% PVA-PBS (w/v) and Rhod-2 fluorescence was measured using an iRiS^{TM} digital cell imaging system (Logos Biosystems, Anyang, Korea). Each sample was washed three times in 0.1% PVA-PBS. Washed presumptive zygotes were cultured in 50 μl of IVC medium mixed with 5 μM Mito-SOX (red fluorescence; Life Technologies, Carlsbad, CA, USA) under mineral oil at 37°C for 30 min. To confirm the mitochondria localization, embryos cultured in 50 μl of IVF medium were mixed with 4 μg/ml Mito-Tracker (Cell Signaling Technology, Danvers, MA, USA) at 38.5ºC for 20 min. Each sample was washed three times in 0.1% PVA-PBS (Supplementary Fig. 5: online only). Mito-Tracker (green) and Mito-SOX (red)-positive cytoplasm in cells were detected using an iRiS^{TM} digital cell imaging system (Logos Biosystems).

Assessment of cellular apoptosis in porcine blastocysts

Blastocysts that developed after RR or histamine treatment during IVF were fixed in 4% paraformaldehyde in PBS for detection of apoptosis by terminal deoxynucleotidyl transferase-mediated dUDP

nick-end labeling (TUNEL) using an In Situ Cell Death Detection Kit (Roche Diagnostics, Mannheim, Germany) according to the manufacturer's instructions. Blastocysts were permeabilized using 0.5% (v/v) Triton X-100 for 30 min at 4°C. The fixed blastocysts were incubated in TUNEL reaction medium for 1 h at 38.5°C, then washed three times with 0.1% PVA-PBS and mounted on slides with mounting solution containing 1.5 μg/ml of 4',6-diamidino-2-phenylindole (DAPI; Vector Laboratories, Burlingame, CA, USA). DAPI-labeled or TUNEL-positive nuclei were examined using the forementioned iRiS™ digital cell imaging system following TUNEL assay and DAPI staining, and the number of apoptotic nuclei and total number of nuclei were counted.

Analysis of MMP and ATP production assay

Fertilized oocytes at 3 h or 6 h after IVF and mature oocytes after 44 h of IVM were washed three times in 0.1% PVA-PBS (v/v) and incubated in 50 μl of IVC medium containing the JC-1 kit (1:100 dilution; Cayman Chemical, MI, USA) under mineral oil at 37°C for 30 min. Washed fertilized oocytes at 3 h or 6 h after IVF and matured oocyte after 44 h of IVM were fixed in 2.5% glutaraldehyde/PBS (v/v) solution for 1 h at room temperature. Embryos were washed three times in 0.1% PVA-PBS and examined using the forementioned iRiS™ digital cell imaging system. MMP assessed as the ratio of red fluorescence to green fluorescence [17]. ATP was determined in matured and fertilized oocytes using an ATP determination kit (Invitrogen, Carlsbad, CA, USA) as previously described [16]. Standard solution was prepared according to the instructions of the manufacturer. One hundred embryos were homogenized with 10 μl RIPA buffer and 90 μl standard buffer was added. Each 100 μl that was prepared was added to a white 96-well plate and incubated for 10 min at room temperature. Luminescence intensity was measured using an InfiniteM200pro luminometer (Tecan, Männedorf, Switzerland).

Protein extraction and western blot analysis

Total protein was extracted from 50 to 60 mature and fertilized oocytes in ice-cold PRO-PREP protein lysis buffer (iNtRON Biotechnology, Daejeon, Korea). Samples were separated by 10% to 12% sodium dodecyl sulfate-polyacrylamide gel electrophoresis (SDS-PAGE) and the separated proteins were transferred to pure nitrocellulose membranes (Pall Life Sciences, Port Washington, NY, USA). After blocking overnight with 5% non-fat milk at 4°C, the membranes were incubated with primary antibodies to β-actin (1:5000 dilution; Santa Cruz Biotechnology, Santa Cruz, CA, USA) or mito-Ca^{2+} uptake 1 (MICU1) (1:4000 dilution, Abcam). The membranes were then incubated with secondary horseradish peroxidase (HRP)-conjugated anti-mouse IgG (1:5000 dilution; Thermo Fisher Scientific, Waltham, MA, USA) or anti-goat IgG (1:5000 dilution; AB Frontier, Seoul, Korea) for 1 h at room temperature and washed with Tris-buffered saline containing 0.1% Tween 20 (TBST) buffer. Antibody binding was detected using a Bright™ enhanced chemiluminescence (ECL) Kit (Advansta, San Jose, CA, USA) according to the manufacturer's instructions. Protein content was determined using Fusion Solo software (Vilber Lourmat, Collégien, France). Band intensities were quantified by densitometry using ImageJ software (NIH, Bethesda, MD, USA). Intensity of the protein bands was normalized relative to that of β-actin. The quantitative analysis was performed for three independent experiments.

Statistical analyses

All measurements were made in triplicate. All percentage data obtained are presented as the mean ± standard deviation (SD). Western blot and ATP contents are presented as the standard error of the mean (SEM). The results were analyzed using one-way ANOVA followed by Bonferroni's and Dunnett's multiple comparison test and *t*-test. Histogram values of densitometry analysis were obtained using ImageJ (NIH). All data were obtained using GraphPad Prism 5.0 (GraphPad, San Diego, CA, USA). Differences were considered significant at * $P < 0.05$, ** $P < 0.01$, and *** $P < 0.001$.

Results

Evaluation of mito-Ca^{2+} in presumptive porcine zygotes treated with RR during IVF

Rhod-2, which detects mito-Ca^{2+}, was used to analyze the expression pattern of mito-Ca^{2+} in fertilized oocytes 6 h after IVF as previously described [13]. Changes of mito-Ca^{2+} were assessed in mature oocytes (44 h following IVM) and fertilized oocytes (6 h following IVF). As shown in Supplementary Fig. 3 (online only), the Rhod-2 fluorescence intensity of presumptive zygotes was significantly increased ($P < 0.05$) compared with mature oocytes. For porcine zygotes examined 3 h after IVF, the MICU1 protein levels were increased but were not significantly different from the levels in matured oocytes. In addition, the protein expression of MICU1 was higher in presumptive zygotes after IVF than in mature oocytes, especially in zygotes at 6 h after IVF ($P < 0.05$). Based on these results, presumptive zygotes at 6 h after IVF as a non-treated group were used for the subsequent experiments.

The red fluorescence intensity of Rhod-2 was significantly decreased ($P < 0.01$) in 20 μM RR-treated presumptive zygotes compared with the other groups (Fig. 1A). The protein expression of MICU1 was significantly decreased ($P < 0.001$) in presumptive zygotes treated with 20 μM RR (Fig. 1B). These results confirmed that mito-Ca^{2+} levels in presumptive zygotes were decreased in 20 μM RR-treated group during the 6 h following IVF.

Mitochondrial functions and superoxide production in RR-treated presumptive porcine zygotes during IVF

Changes of mitochondrial functions and mitochondrial-derived reactive oxygen species (mito-ROS) production in RR-treated and non-treated group were measured using ATP determination kit, JC-1 staining, and Mito-SOX staining, respectively. ATP contents were significantly increased ($P < 0.01$) by treatment with 20 μM RR compared with 10 μM RR-treated and non-treated groups (Fig. 2A). MMP was increased in 20 μM RR-treated presumptive zygotes ($P < 0.05$) compared with control or RR (10 μM)-treated presumptive zygotes 6 h after IVF (Fig. 2B). Mito-SOX red fluorescence intensity significantly decreased (10 μM RR: $P < 0.05$ and 20 μM RR: $P < 0.01$) in RR-treated groups compared with non-treated groups (Fig. 2C). And, we investigated the changes of mitochondria localization using Mito-Tracker staining in 10 and 20 μM RR-treated presumptive zygotes. No significant difference of Mito-Tracker green fluorescence intensity was found between the non-treatment and RR treated groups

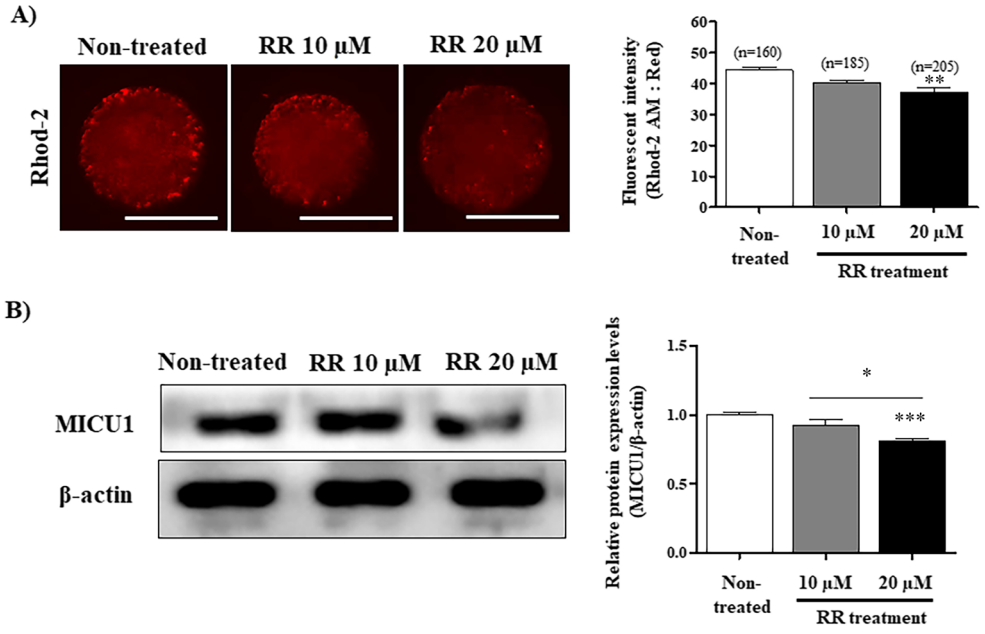

Fig. 1. Identification of mito-Ca^{2+} level using Rhod2 staining and mito-Ca^{2+} uptake 1 (MICU1) expression analysis in porcine presumptive zygotes after ruthenium red (RR) treatment during *in vitro* fertilization (IVF). (A) Rhod-2 fluorescence intensity in 10 and 20 μM RR-treated presumptive zygotes after 6 h IVF. (B) Western blot analysis was performed to evaluate the level of MICU1 in the RR-treated presumptive zygotes. The relative level of MICU1 protein was obtained after normalization with β-actin level. The histogram values of densitometry analysis were obtained using Image J software. The bars represent the mean of three independent experiments ± SEM (50–60 zygotes per group). * $P < 0.05$; Dunn's Multiple Comparison Test compared to non-treated group. Scale bar denotes 100 μm.

(Supplementary Fig. 5).

Effects of RR treatment during IVF on blastocyst development and quality

To investigate the effects of RR treatment during IVF on early embryonic development to the blastocyst stage, we examined the blastocyst developmental rate, expanded blastocyst formation, and cellular apoptosis using the TUNEL assay. First, we investigated the cleavage and blastocyst development rates of porcine embryos after various concentrations (5, 10, 20, and 40 μM) of RR treatment for IVF (Supplementary Fig. 4: online only). Interestingly, the blastocyst developmental rate was significantly improved in the 20 μM RR-treated group compared with other groups (Table 1; 20 μM RR-treated groups: 32.2 ± 4.3% *vs*. non-treated group: 24.1 ± 2.4% and 10 μM RR-treated group: 24.8 ± 4.9%; $P < 0.05$). However, the blastocyst development rate was not changed in 40 μM RR-treated oocytes compared with the non-treated group (Supplementary Fig. 4: online only). And, expanded blastocyst rate also significantly increased ($P < 0.01$) in 20 μM RR-treated zygotes compared with other groups (Fig. 3A). Next, as expected, the expanded blastocyst production was significantly increased ($P < 0.05$) in developed blastocysts derived from 20 μM RR-treated zygotes (Fig. 3B). Finally, the TUNEL assay confirmed cell death as a result of cellular apoptosis in porcine blastocysts following treatment with 10 or 20 μM RR. As shown in Fig. 3B, the number of nuclei in blastocysts in the 20 μM RR-treated group was significantly greater ($P < 0.05$) that of the non-treated group. Also, the percentage of TUNEL-positive cells in blastocysts of the 20 μM RR-treated group was significantly lower ($P < 0.05$) than that of the other groups.

Histamine-mediated increase of mito-Ca^{2+} levels in presumptive porcine zygote after IVF

Histamine is a reagent that is used in research related to mito-Ca^{2+} [18]. To investigate the effects of histamine treatment during IVF on early embryonic development, we investigated the development rate in blastocysts that developed from zygotes treated with 100 nM histamine. Rhod-2 fluorescence intensity and MICU1 protein expression were measured in the histamine-treated oocytes during IVF. The fluorescence intensity of Rhod-2 was significantly increased ($P < 0.05$) in the histamine-treated group compared to that in the non-treated group (Fig. 4A). The MICU1 protein level was significantly increased ($P < 0.01$) in the histamine-treated group compared with the level in the non-treated group (Fig. 4B).

Effects of histamine-mediated induction of mito-Ca^{2+} during IVF on blastocyst development and quality

The blastocyst developmental rate was significantly decreased in the 100 nM histamine-treated group compared with that in the non-treated group (29.0 ± 3.4% *vs*. 18.6 ± 5.3%; $P < 0.05$; Table 2). The expanded blastocyst rate was also significantly decreased in the 100 nM histamine-treated group compared to the rate in the non-treated group ($P < 0.05$; Fig. 5A). As shown in Fig. 5B, the number of nuclei in blastocysts were significantly decreased ($P < 0.05$) in the 100 nM histamine-treated group, while the percentage

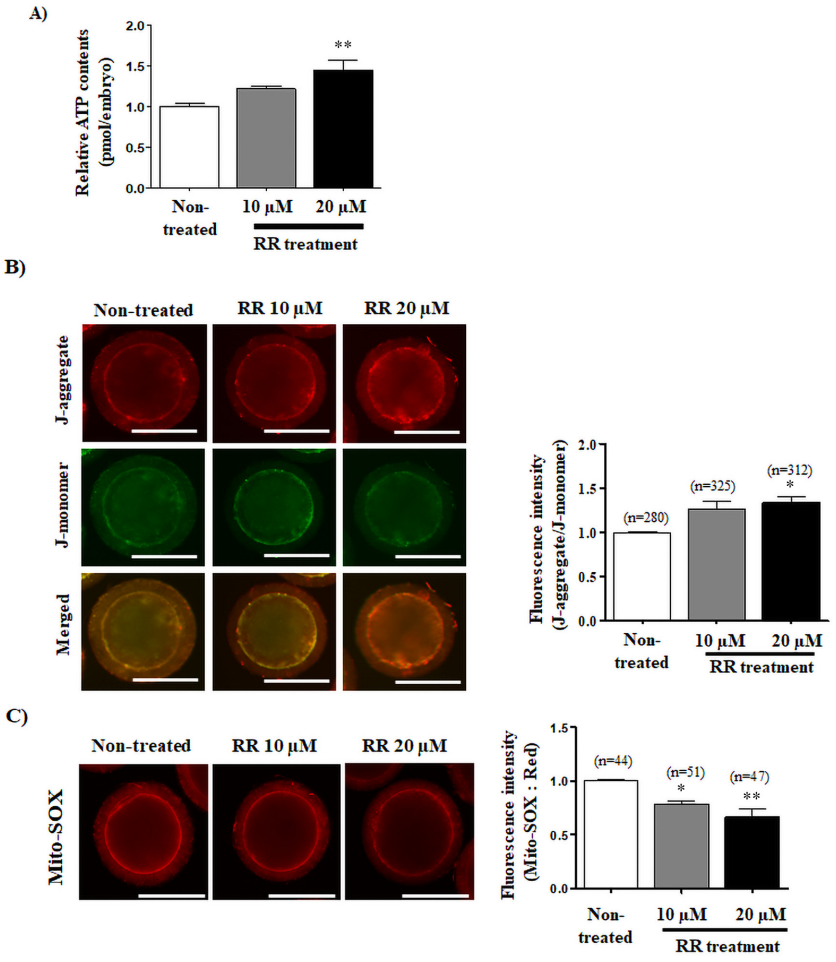

Fig. 2. Changes of mitochondrial functions in porcine presumptive zygotes by ruthenium red (RR) treatment. (A) ATP contents were measured using the ATP determination kit (Invitrogen) with a microplate reader. (B) Expression of J-aggregate (red) and J-monomer (green) to confirm the mitochondrial membrane potential (MMP) using JC-1 staining and confocal microscopy. (C) Superoxide mitochondria-derived reactive oxygen species (ROS) was detected by Mito-SOX staining and is depicted as a histogram of JC-1 obtained using Image J software. * $P < 0.05$ and ** $P < 0.01$; One-way - ANOVA, Dunn's Multiple Comparison Test compared to non-treated group. The data in the bar graph represent mean ±standard error of the mean (SEM). Scale bar denotes 100 μm.

Table 1. Comparison of blastocyst development from porcine presumptive zygotes treated with ruthenium red (RR) during *in vitro* fertilization (IVF)

Groups	No. of embryos cultured	% of embryos cleaved (n)	% of blastocysts (n)
Non-treated	224	84.4 ± 5.8 (189)	24.1 ± 2.4 (54) [a]
10 μM RR	191	85.1 ± 10.6 (165)	24.8 ± 4.9 (49) [ab]
20 μM RR	211	86.6 ± 7.5 (184)	32.2 ± 4.7 (69) [b]

This experiment was replicated three times. The data are expressed as mean ± SD. [ab] Different superscript letters denote a significant difference compared with other groups ($P < 0.05$).

of TUNEL-positive cells in histamine-treated blastocyst populations was significantly increased ($P < 0.05$).

Discussion

Our study is the first to describe the positive effects of RR in improving the developmental capacity to the blastocyst stage in pigs. We confirmed higher mito-Ca^{2+}levels and increased MICU1 protein expression in presumptive zygotes 6 h after IVF. We also confirmed that the use of RR on fertilized oocyte for IVF improves blastocyst development and quality.

RR inhibits Ca^{2+} from entering mitochondria through MCU com-

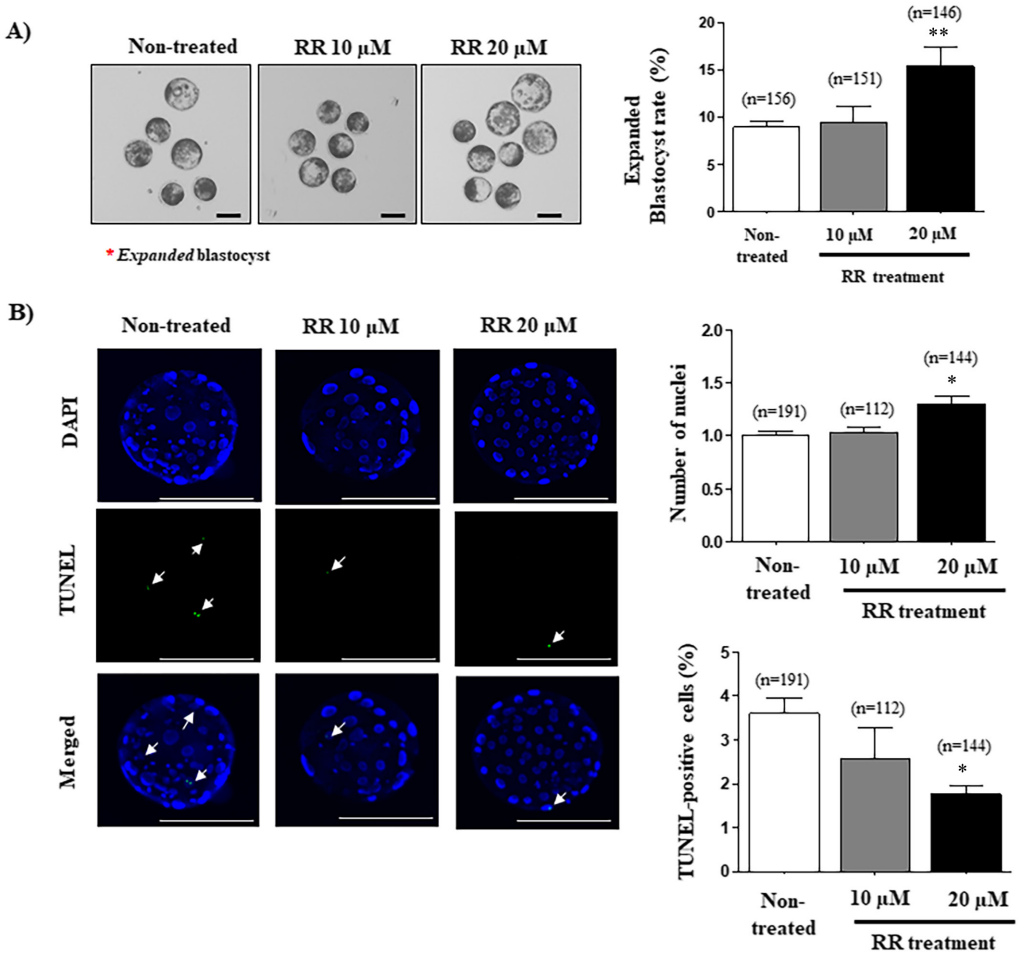

Fig. 3. Effects of reducing mito-Ca^{2+} in ruthenium red (RR)-treated presumptive porcine zygotes on blastocyst development and quality. (A) Formation of expanded blastocysts was measured by optical microscopy in RR-treated and non-treated groups. The red stars indicate expanded blastocysts. (B) Nuclei (blue) and terminal deoxynucleotidyl transferase-mediated dUDP nick-end labeling (TUNEL)-positive cells (green) of RR-treated blastocysts visualized using the iRiS^{TM} image system. The left histogram is the total number of DAPI-stained nuclei in blastocysts and the right histogram is the percentage of TUNEL-positive cells in blastocysts. The data in the bar graph represent the means ± standard error of the mean (SEM) from three independent experiments; * $P < 0.05$ and ** $P < 0.01$; One-way ANOVA, Dunn's Multiple Comparison Test compared to non-treated group. Scale bar denotes 100 μm.

plexes from the cytoplasm in rats [19]. MICU1 combines with the DIME domain to activate MCU (Ca^{2+} uniporter protein, mitochondrial) that has been inhibited by RR [20], while RR inhibits MCU that has been activated by MICU1 in HeLa cells [21]. Among MCU subunits, MICU1 is essential for Ca^{2+} homeostasis in mitochondria as a gatekeeper to MCU-mediated Ca^{2+} uptake in HeLa cells [22]. Additionally, the MICU1 is selectively regulated in a proteasome-dependent manner in Parkinson's disease, as well as lead to a brain and muscle disorder linked to mito- Ca^{2+} signaling [23]. As shown in Fig. 1A, we observed a reduced level of mito-Ca^{2+} based on Rhod-2 fluorescence in RR-treated presumptive zygotes after IVF. Our previous study demonstrated the evidence that considerable relevance of Rhod-2 expression pattern on oocyte maturation capacity or quality during IVM. [13]. The reduced fluorescence expression of Rhod-2 in porcine zygote exposed to RR can be inferred that the zygote quality or fertilization capacity of porcine oocyte has helped to improve. Protein expression of MICU1 was also decreased following RR treatment during IVF (Fig. 1B). The present findings provide the first evidence of MICU1 protein expression associated with RR treatment in porcine oocytes during IVF. We suggest that RR plays a role as a competitive inhibitor of MICU1, and also decreases MICU1 protein expression.

Enhancement of MICU1 protein expression is related to increased mito-Ca^{2+} levels [24]. As shown in Supplementary Fig. 3, we confirmed that the mito-Ca^{2+} level was increased in presumptive zygotes 6 h after IVF. A previous study showed that mito-Ca^{2+} accumulation is associated with mitochondrial dysfunctions, such as disruption of cytoplasmic Ca^{2+} homeostasis, in neurodegenerative disorders [25]. Thus, the proposed potential effects of RR-mediated change in mito-Ca^{2+} homeostasis might be necessary for the improved fertilization capacity during IVF.

No study has reported the relationship between the regulation of

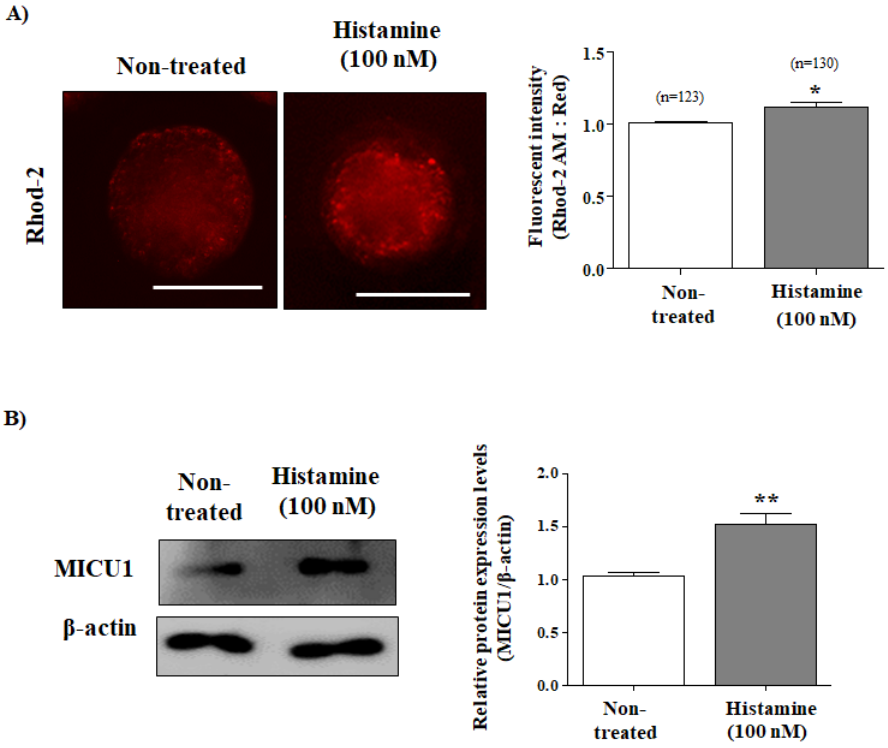

Fig. 4. Changes in mito-Ca^{2+} of porcine presumptive zygotes after histamine treatment during *in vitro* fertilization (IVF). (A) Rhod-2 fluorescence intensity was investigated in 100 nM histamine-treated presumptive zygotes 6 h after IVF. (B) Western blot analysis was performed to evaluate the level of mito-Ca^{2+} uptake 1 (MICU1) in presumptive zygotes treated with 100 nM histamine. The relative levels of MICU1 protein were obtained after normalization to the level of β-actin. The histogram values of densitometry analysis were obtained using Image J software. The bars represent the means of three independent experiments ± standard error of the mean (SEM) (50–60 zygotes per group); * $P < 0.05$ and ** $P < 0.01$; *t*-test compared to non-treated group. Scale bar denotes 100 μm.

mito-Ca^{2+} by RR and the maintenance of mitochondrial functions in porcine zygotes after IVF. We investigated the positive effect of mito-Ca^{2+} reduction by RR on maintenance of mitochondrial functions in presumptive porcine zygotes 6 h after IVF (Fig. 2). To assess the mitochondrial quality in these zygotes, we identified increases in ATP production and MMP, and decreased mitochondria-derived superoxide generation in RR-treated porcine oocytes during IVF. The ATP content of mature oocytes is directly related to fertilization ability and blastocyst development in human embryos [26]. Also, the MMP is associated with ATP production, indicating the health and metabolic status of mitochondria [27].

In mice oocytes, mitochondria with high MMP convert superoxide to hydrogen peroxide (H_2O_2), which then diffuses into the cytoplasm. The result is a low level of mitochondria-derived ROS (mito-ROS) [28]. However, damage by mito-Ca^{2+} accumulation in post-ischemic heart failure of mice causes mitochondrial dysfunctions, resulting in reduced ATP production and ROS production [24]. Also, our results suggest that the mito-Ca^{2+} reduction by RR treatment improves mitochondrial functions through the avoidance of severe mito-Ca^{2+} accumulation in porcine presumptive zygotes after IVF. In addition, the analyses of RR-treated oocytes and zygotes revealed the reduction of mito-ROS during IVF (Fig. 2C). Our previous study demonstrated that high levels of mito-ROS production can induce reduced oocyte quality, meiotic maturation, and cumulus cell expansion in pigs during IVM [17]. These findings suggest that the reduction of mito-Ca^{2+} by RR treatment is related to mito-ROS production in porcine oocytes and zygotes during IVM and IVF.

The maintenance of mitochondria function is important in blastocyst development [29]. The rate of expanded blastocysts, total cell number, and TUNEL-positive cells in porcine blastocysts are used to compare the qualities of blastocysts [17]. Presently, blastocyst development and quality were higher in 20 μM RR-treated presumptive zygotes (Table 1 and Fig. 3), which had the most improved mitochondrial function at 6 h IVF (Fig. 2). These results suggest that reduction of mito-Ca^{2+} by RR in porcine presumptive zygotes after IVF improves blastocyst development by enhancing mitochondrial functions. However, additional studies are needed to elucidate the mechanism by RR-derived mito-Ca^{2+} during IVF progression, which acts to regulate preimplantation embryo development in porcine embryos. Therefore, as a contrast to RR, we used histamine to up-regulate mito-Ca^{2+} in porcine oocytes during IVF.

Treatment with histamine increases mito-Ca^{2+} through the MCU in HeLa cells [30]. To confirm whether the presently observed RR-mediated reduction of mito-Ca^{2+} enhanced blastocyst competence, we investigated the roles of histamine as a mito-Ca^{2+} inhibitor. As shown in Fig. 4, both the protein level of MICU1 and Rhod-2 expression

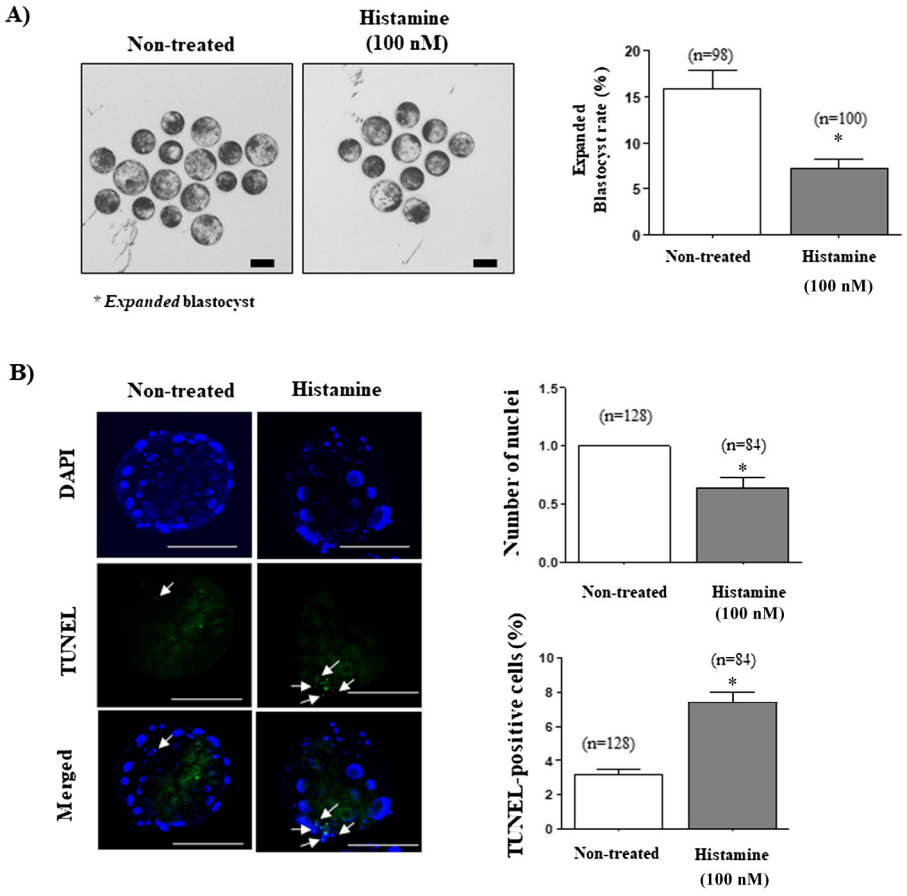

Fig. 5. Investigation of blastocyst development and quality from porcine presumptive zygotes treated with histamine during *in vitro* fertilization (IVF). (A) Expanded blastocyst production was observed using optical microscopy. The red stars indicate expanded blastocysts. (B) Nuclei (blue) and terminal deoxynucleotidyl transferase-mediated dUDP nick-end labeling (TUNEL)-positive cells (green) of blastocysts were visualized using the iRiS^{TM} image system. The left histogram is the number of DAPI-stained nuclei and the right histogram is the percentage of TUNEL-positive cells. The data in the bar graph represent the mean ± standard error of the mean (SEM) from three independent experiments; * $P < 0.05$; *t*-test was used. Scale bar denotes 100 μm. White arrows indicate the apoptotic nuclei in TUNEL positive cells.

Table. 2. Comparison of blastocyst development from porcine presumptive zygotes treated with histamine during *in vitro* fertilization (IVF)

Histamine treatment	No. of embryos culture	% of embryos cleaved (n)	% of blastocysts (n)
Non-treated	161	83.1 ± 3.5 (135)	29.0 ± 3.4 (47) [a]
100 nM	163	74.7 ± 8.0 (123)	18.6 ± 5.3 (30) [b]

This experiment was replicated three times. The data are expression as means ± SD. [ab] Different superscript letters denote a significant difference compared with other groups ($P < 0.05$).

were significantly increased in histamine-treated presumptive zygotes 6 h after IVF. As shown in Table 2 and Fig. 5, in contrast to the RR treatment group, the development and quality of blastocysts in the histamine-treated group were significantly lower than the levels in the non-treated group. These results suggest that the increase in the mito-Ca^{2+} level by histamine during IVF may have induced problems in developmental competence and quality of blastocysts due to mitochondrial dysfunction or mito-Ca^{2+} accumulation. Therefore, the reduction of blastocyst development in histamine-treated presumptive zygotes indicates that the regulation of mito-Ca^{2+} during IVF was closely related to blastocyst development.

The collective data confirm the interaction between the RR-mediated reduction in mito-Ca^{2+} and improved mitochondria functions in presumptive zygotes after IVF, and demonstrate the association with further blastocyst development. Figure 6 provides a graphical summary. Moreover, we generally observed the maintenance of a high level of mito-Ca^{2+} in mature oocytes and fertilized presumptive zygotes *in vitro*. This phenomenon could be mitigated by RR treatment.

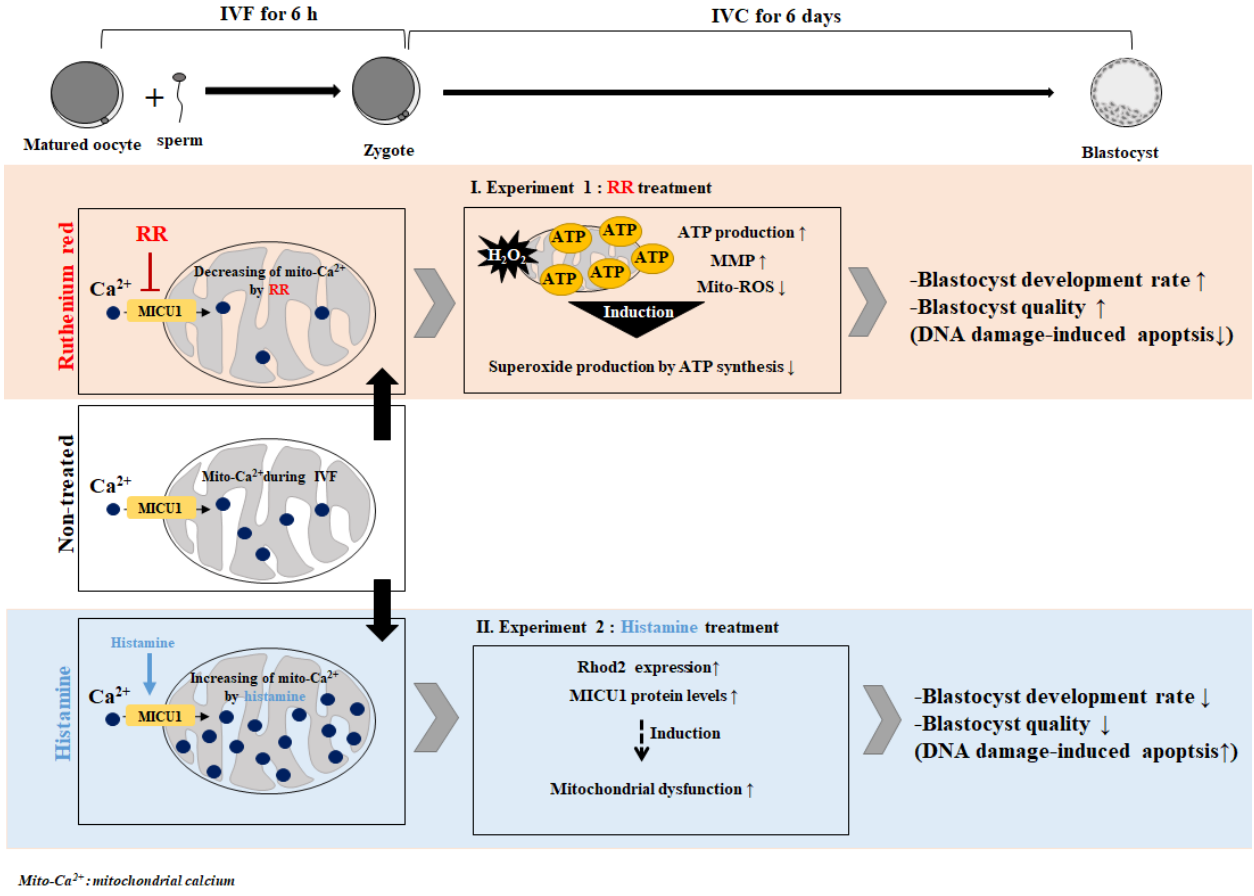

Fig. 6. Graphical summary. The study sought i) to confirm the relationship between ruthenium red (RR)-mediated reduced mito-Ca^{2+} levels and improved mitochondrial functions in fertilized oocytes after *in vitro* fertilization (IVF), and ii) to demonstrate the interaction between mito-Ca^{2+} regulation by RR (mito-Ca^{2+} indicator) or histamine (mito-Ca^{2+} inhibitor) based on mitochondrial function in blastocyst development and morphological competence of porcine presumptive zygotes. The findings show that the regulation of mito-Ca^{2+} in RR-treated porcine presumptive zygotes improves blastocyst development and quality by promoting mitochondrial functions.

Contrary to RR treatment, we demonstrated that increasing mito-Ca^{2+} levels by histamine in presumptive zygotes affected the reduction of both blastocyst development and quality in pigs. Based on these results, we conclude that the regulation of mito-Ca^{2+} by RR treatment during IVF in porcine presumptive zygotes plays important roles in mitochondrial functions and blastocyst developmental competence *in vitro*.

Conflict of interests: The authors declare no competing interests.

Acknowledgments

This research was supported by the Basic Science Research Program through the National Research Foundation of Korea (NRF-2018R1D1A1B07044173, NRF-2018R1C1B002922 and NRF-2019R1A2C1085199) and Cooperative Research Program for Agriculture Science and Technology Development (PJ01269503) through the Ministry of Education, the Ministry of Science and ICT, and the Rural Development Administration, Republic of Korea.

References

1. **Dumollard R, Marangos P, Fitzharris G, Swann K, Duchen M, Carroll J.** Sperm-triggered [Ca2+] oscillations and Ca2+ homeostasis in the mouse egg have an absolute requirement for mitochondrial ATP production. *Development* 2004; **131**: 3057–3067. [Medline] [CrossRef]
2. **Stanika RI, Pivovarova NB, Brantner CA, Watts CA, Winters CA, Andrews SB.** Coupling diverse routes of calcium entry to mitochondrial dysfunction and glutamate excitotoxicity. *Proc Natl Acad Sci USA* 2009; **106**: 9854–9859. [Medline] [CrossRef]
3. **Tripathi A, Chaube SK.** High cytosolic free calcium level signals apoptosis through mitochondria-caspase mediated pathway in rat eggs cultured in vitro. *Apoptosis* 2012; **17**: 439–448. [Medline] [CrossRef]
4. **Dumollard R, Duchen M, Carroll J.** The role of mitochondrial function in the oocyte and embryo. *Curr Top Dev Biol* 2007; **77**: 21–49. [Medline] [CrossRef]
5. **Pinton P, Giorgi C, Siviero R, Zecchini E, Rizzuto R.** Calcium and apoptosis: ER-mitochondria Ca2+ transfer in the control of apoptosis. *Oncogene* 2008; **27**: 6407–6418. [Medline] [CrossRef]
6. **De Stefani D, Raffaello A, Teardo E, Szabò I, Rizzuto R.** A forty-kilodalton protein of the inner membrane is the mitochondrial calcium uniporter. *Nature* 2011; **476**: 336–340. [Medline] [CrossRef]
7. **Mishra J, Jhun BS, Hurst S, O-Uchi J, Csordás G, Sheu SS.** The mitochondrial Ca^{2+} uniporter: structure, function, and pharmacology. *Handb Exp Pharmacol* 2017; **240**: 129–156. [Medline] [CrossRef]
8. **Dumollard R, Duchen M, Sardet C.** Calcium signals and mitochondria at fertilisation.

Semin Cell Dev Biol 2006; **17**: 314–323. [Medline] [CrossRef]

9. **Xu D, Wu L, Jiang X, Yang L, Cheng J, Chen H, Hua R, Geng G, Yang L, Li Q.** SIRT2 inhibition results in meiotic arrest, mitochondrial dysfunction, and disturbance of Redox homeostasis during bovine oocyte maturation. *Int J Mol Sci* 2019; **20**: 20. [Medline]
10. **Jeong SY, Seol DW.** The role of mitochondria in apoptosis. *BMB Rep* 2008; **41**: 11–22. [Medline] [CrossRef]
11. **Bowser DN, Minamikawa T, Nagley P, Williams DA.** Role of mitochondria in calcium regulation of spontaneously contracting cardiac muscle cells. *Biophys J* 1998; **75**: 2004–2014. [Medline] [CrossRef]
12. **Zhao L, Lu T, Gao L, Fu X, Zhu S, Hou Y.** Enriched endoplasmic reticulum-mitochondria interactions result in mitochondrial dysfunction and apoptosis in oocytes from obese mice. *J Anim Sci Biotechnol* 2017; **8**: 62. [Medline] [CrossRef]
13. **Jegal HG, Park HJ, Kim JW, Koo DB.** Confirmation of mitochondrial specific Rhod-2 expression patterns in matured and fertilized porcine oocyte in vitro. *Ann Anim Resour Sci* 2019; **30**: 8–17. [CrossRef]
14. **Malécot CO, Bito V, Argibay JA.** Ruthenium red as an effective blocker of calcium and sodium currents in guinea-pig isolated ventricular heart cells. *Br J Pharmacol* 1998; **124**: 465–472. [Medline] [CrossRef]
15. **Petters RM, Wells KD.** Culture of pig embryos. *J Reprod Fertil Suppl* 1993; **48**: 61–73. [Medline]
16. **Yang SG, Park HJ, Kim JW, Jung JM, Kim MJ, Jegal HG, Kim IS, Kang MJ, Wee G, Yang HY, Lee YH, Seo JH, Kim SU, Koo DB.** Mito-TEMPO improves development competence by reducing superoxide in preimplantation porcine embryos. *Sci Rep* 2018; **8**: 10130. [Medline] [CrossRef]
17. **Hua S, Zhang H, Song Y, Li R, Liu J, Wang Y, Quan F, Zhang Y.** High expression of Mfn1 promotes early development of bovine SCNT embryos: improvement of mitochondrial membrane potential and oxidative metabolism. *Mitochondrion* 2012; **12**: 320–327. [Medline] [CrossRef]
18. **Jou MJ, Peng TI, Sheu SS.** Histamine induces oscillations of mitochondrial free Ca2+ concentration in single cultured rat brain astrocytes. *J Physiol* 1996; **497**: 299–308. [Medline] [CrossRef]
19. **Kannurpatti SS, Biswal BB.** Mitochondrial Ca2+ uniporter blockers influence activation-induced CBF response in the rat somatosensory cortex. *J Cereb Blood Flow Metab* 2008; **28**: 772–785. [Medline] [CrossRef]
20. **Vecellio Reane D, Vallese F, Checchetto V, Acquasaliente L, Butera G, De Filippis V, Szabò I, Zanotti G, Rizzuto R, Raffaello A.** A MICU1 splice variant confers high sensitivity to the mitochondrial Ca^{2+} uptake machinery of skeletal muscle. *Mol Cell* 2016; **64**: 760–773. [Medline] [CrossRef]
21. **Paillard M, Csordás G, Huang KT, Várnai P, Joseph SK, Hajnóczky G.** MICU1 interacts with the D-ring of the MCU pore to control its Ca^{2+} flux and sensitivity to Ru360. *Mol Cell* 2018; **72**: 778–785.e3. [Medline] [CrossRef]
22. **Mallilankaraman K, Doonan P, Cárdenas C, Chandramoorthy HC, Müller M, Miller R, Hoffman NE, Gandhirajan RK, Molgó J, Birnbaum MJ, Rothberg BS, Mak DO, Foskett JK, Madesh M.** MICU1 is an essential gatekeeper for MCU-mediated mitochondrial $Ca^{(2+)}$ uptake that regulates cell survival. *Cell* 2012; **151**: 630–644. [Medline] [CrossRef]
23. **Matteucci A, Patron M, Vecellio Reane D, Gastaldello S, Amoroso S, Rizzuto R, Brini M, Raffaello A, Calì T.** Parkin-dependent regulation of the MCU complex component MICU1. *Sci Rep* 2019; **9**: 4665. [Medline] [CrossRef]
24. **Antony AN, Paillard M, Moffat C, Juskeviciute E, Correnti J, Bolon B, Rubin E, Csordás G, Seifert EL, Hoek JB, Hajnóczky G.** MICU1 regulation of mitochondrial Ca^{2+} uptake dictates survival and tissue regeneration. *Nat Commun* 2016; **7**: 10955. [Medline] [CrossRef]
25. **Liao Y, Dong Y, Cheng J.** The function of the mitochondrial calcium uniporter in neurodegenerative disorders. *Int J Mol Sci* 2017; **18**: E248. [Medline] [CrossRef]
26. **Van Blerkom J, Davis PW, Lee J.** ATP content of human oocytes and developmental potential and outcome after in-vitro fertilization and embryo transfer. *Hum Reprod* 1995; **10**: 415–424. [Medline] [CrossRef]
27. **Vergun O, Reynolds IJ.** Fluctuations in mitochondrial membrane potential in single isolated brain mitochondria: modulation by adenine nucleotides and Ca2+. *Biophys J* 2004; **87**: 3585–3593. [Medline] [CrossRef]
28. **Komatsu K, Iwase A, Mawatari M, Wang J, Yamashita M, Kikkawa F.** Mitochondrial membrane potential in 2-cell stage embryos correlates with the success of preimplantation development. *Reproduction* 2014; **147**: 627–638. [Medline] [CrossRef]
29. **Lee KS, Huh S, Lee S, Wu Z, Kim AK, Kang HY, Lu B.** Altered ER-mitochondria contact impacts mitochondria calcium homeostasis and contributes to neurodegeneration in vivo in disease models. *Proc Natl Acad Sci USA* 2018; **115**: E8844–E8853. [Medline] [CrossRef]
30. **Liao Y, Hao Y, Chen H, He Q, Yuan Z, Cheng J.** Mitochondrial calcium uniporter protein MCU is involved in oxidative stress-induced cell death. *Protein Cell* 2015; **6**: 434–442. [Medline] [CrossRef]